

Control of the wavelength dependent thermo-optic coefficients in structured fibres

H.R. Sørensen¹, J. Canning², J. Lægsgaard¹, K. Hansen³

¹Research Center COM, Technical University of Denmark, Ørstedes Plads, Building 345 V, DK-2800 Kgs. Lyngby Denmark

²Optical Fibre Technology Centre, ATP, University of Sydney, Sydney, NSW 1430, Australia.

³Crystal Fibre, Blokken 84, DK-3460 Birkerød Denmark

Abstract: By controlling the fibre geometry, the fraction of optical field within the holes and the inserted material of a photonic crystal fibre, we demonstrate that it is possible to engineer any arbitrary wavelength-dependent thermo-optic coefficient. The possibility of making a fibre with a zero temperature dependent thermo-optic coefficient, ideal for packaging of structured fibre gratings, is proposed and explored.

©2006 Optical Society of America

OCIS codes: (050.2770) Gratings; (060.2290) Fiber materials; (160.5320) Photorefractive materials; (999.9999) photonic crystal fibres; (999.9999) photonic amorphous fibres; (999.9999) air-structured fibres; (999.9999) Fresnel fibres; (999.9999) air-clad fibres; (999.9999) thermo-optic coefficient; (999.9999) organic liquids; (999.9999) packaging; (999.9999) alkanes; (999.9999) *n*-heptane; (999.9999) perfluoroheptane; (999.9999) sensors; (999.9999) composites; (999.9999) structured devices; (999.9999) microfluidics; (999.9999) microtechnology

References and links

1. E.A.J. Marcatili, "Air clad optical fiber waveguide," US patent 3,712,705 (1973).
2. A. Bjarklev, J. Broeng, A.S. Bjarklev, *Photonic Crystal Fibres*, (Kluwer Academic Publishers, 2003)
3. J. Canning, "Diffraction-free mode generation and propagation in optical waveguides," *Opt. Comm.* **207** (1-6) 35-39 (2002)
4. C. Martelli, J. Canning, N. Groothoff and K. Lyytikäinen, "Strain and temperature characterization of photonic crystal fiber Bragg gratings," *Opt. Lett.* **30**, 1785, (2005)
5. G.P. Agrawal, "*Fiber-Optic Communication systems 2nd edition*," (Wiley-Interscience 1997)
6. S. G. Johnson and J. D. Joannopoulos, "Block-iterative frequency-domain methods for Maxwell's equations in a planewave basis," *Opt. Express* **8**, 173-190 (2001)
7. *Handbook of Physics and Chemistry*, (CRC Press 1984)
8. H. R. Sørensen, J. B. Jensen, J. Bo Jensen, F. Bruyere, K. P. Hansen, "Practical Hydrogen Loading of Air Silica Fibres," Conf. on Bragg Gratings, Poling and Photosensitivity BGPP2005, Sydney Australia (2005)
9. A. Ito, A. Goto, "Measurements of refractive index for several liquid and its dependence on temperature," *Trans. Jpn. Soc. Mechanical Eng.* **60** (576).2875-2881, (1994).

1. Introduction

Air-structured fibres such as air-clad fibres [1], photonic crystal fibres [2] and Fresnel fibres [3] offer a new approach to engineering optical waveguide properties. This can be done by adjusting the distribution of holes and/or by filling the holes with appropriate materials. An example of the former is the recent demonstration of a quadratic dependence of the effective index versus strain [4]. Given the relationship between the optical mode and its fractional overlap with the holes, sophisticated control of the effective index and associated parameters, can be readily achieved by adjusting the effective composite material made up by the host and hole media. Consequently, by tailoring the presence of air structures within the fibre, the mechanical properties such as strain can be changed whilst not affecting the thermo-optic coefficient, offering a way to discriminate between thermal and strain effects in optical fibres and optical fibre gratings. In contrast, within this paper a simple approach to controlling the thermo-optic coefficient of a photonic to achieve temperature insensitive thermal dependence of refractive index, ideal for simple packaging of components such as photonic crystal fibre

gratings is described. By way of example, we demonstrate the ability of temperature tuning a conventional Bragg grating written into a germanosilicate core air-silica photonic crystal fibre such that its Bragg wavelength decreases as a function of temperature, rather than increases. Further, by controlling the choice of material inserted into the holes and appropriately designing the fibre geometry, it is possible to achieve temperature insensitive thermal

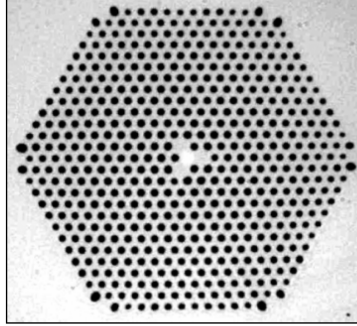


Fig. 1. Optical micrograph of cross-section of photonic crystal fibre. The germanium doping is in the centre rod, placed there during preform stacking.

dependence of refractive index, ideal for simple packaging of components such as photonic crystal fibre gratings.

2. Germanosilicate-doped core photonic crystal fibre

The photonic crystal fibre used in these experiments is shown in Fig. 1 and is available commercially from Crystal Fibre, Denmark. The average core diameter is $2.1\mu\text{m}$ whilst the germanosilicate central core is $(2.1\pm 0.3)\mu\text{m}$. Germanium is added in order to make the fibre photosensitive to conventional grating writing methods that exploit index change triggered by single photon excitation of oxygen deficient centres. The diameter of the surrounding holes is $1\mu\text{m}$ whilst the pitch is $\sim 1.55\mu\text{m}$. This leads to a fill factor of the holes of $FF \sim 0.31$. The measured mode field diameter at $1.55\mu\text{m}$ is quoted to be $(2.8\pm 0.5)\mu\text{m}$.

An analysis of the energy distribution requires an analysis of the wave equation using an expanded dielectric function, $\epsilon(r)$ describing the dielectric constant changes in the different fibre regions. Using a scalar approximation for simplicity, we have the wave equation

$$\nabla^2\psi(r) + k_0^2\epsilon(r)\psi(r) = \beta^2\psi(r) \quad (1)$$

where $\psi(r)$ is the electric or magnetic field function normalized so that

$$\langle \psi(r) \rangle^2 = \int_A \psi(r) \psi(r) dr = 1 \quad (2)$$

and the propagation constant is defined as $\beta = n_{eff} \frac{2\pi}{\lambda}$. From this equation, an expression for the effective index in terms of the field distribution may be derived:

$$n_{eff}^2 = -\left(\frac{\lambda}{2\pi}\right)^2 \int |\nabla\psi(r)|^2 dr + \int \epsilon(r)\psi^2(r) dr. \quad (3)$$

The last term on the right hand side of Eq. (3) corresponds to the averaged value of the dielectric function, whereas the first term on the right hand side is a curvature term that reduces the effective index, especially for long wavelengths. The derivative of the effective index with respect to temperature, however, has a simpler and more intuitive form:

$$\left(\frac{\partial n_{eff}}{\partial T}\right) = (1-\eta_h)\left(\frac{\partial n_{SiO_2}}{\partial T}\right) + \eta_h\left(\frac{\partial n_h}{\partial T}\right) \quad (4)$$

An expression similar to Eq. (4) may be derived in a full-vectorial approach.

Using a full-vectorial plane wave expansion scheme implemented in a freely available software package [6], the ratio of light in the microstructured regions of the fibre, η_h , can be calculated as a function of their refractive index, n_h

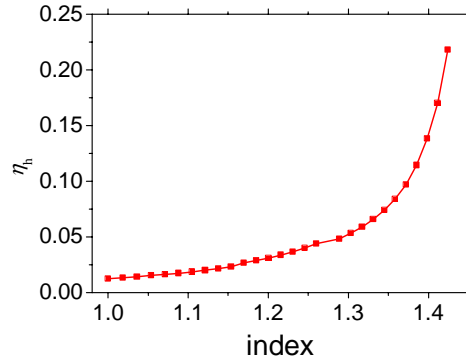


Fig. 2. Fraction of $\lambda=1.5\mu\text{m}$ light in the holes versus the index of the material within the holes.

Figure 2 shows the calculated fraction of energy within the holes for the fibre used here as a function of the index of the material within the holes. For air very little light extends into the holes suggesting any mode properties are dominated by the glass material properties. It is worth noting that if the effective index is calculated using methods applied to conventional step-index fibres where an averaged cladding index is based on the fill-factor weighted average of air-holes and cladding index, then 10% of the light would be situated in the holes. The difference between the 2% found in figure 2 and the 10% is made up of the electrical field shunning the air-hole regions of the fibre, and the fact that the mode field is not circular symmetric and Gaussian in profile due to the complicated shape of the core.

To determine the thermo-optic coefficient of the fibre, the derivative of Eq. (3) yields the intuitive formula in Eq. (4), reflecting the principle of superposition of the fibres individual constituents. For silica $\partial n_{SiO_2}/\partial T \approx 9 \times 10^{-6} \text{ }^\circ\text{C}^{-1}$ at 1550nm [9].

3. Fibre gratings

Gratings were written into the fibre with air ($n_{air} = 1$), *n*-heptane and perfluoroheptane in the holes. In addition to the suitable properties listed in table 1, these liquids, like most organic liquids, have large negative thermo-optic coefficients. For *n*-heptane $dn/dT = -500 \times 10^{-6} \text{ }^\circ\text{C}^{-1}$ at 25°C [7]; we were unable to find any value in the literature for perfluoroheptane. By ensuring our measurements for *n*-heptane agree with the value in the literature, the novel use of gratings in photonic crystal fibres as a practical and simple tool for determining thermo-optic coefficients for material such as perfluoroheptane can also be demonstrated.

Table 1. Properties of *n*-heptane and perfluoroheptane. Values obtained from [6]. No value of absorbance for perfluoroheptane was found. However, generally fluorine displacement of hydrogen in simple organic molecules tends to increase UV transmissivity substantially.

species	absorbance @248nm	m.p. (°C)	b.p. (°C)	density (gcm ⁻³)	index
Heptane CH ₃ (CH ₂) ₅ CH ₃	~0.01	-91	98	0.679	1.38
Perfluoroheptane CF ₃ (CF ₂) ₅ CF ₃	<0.01 (estimated)	-512	83	1.733	1.26

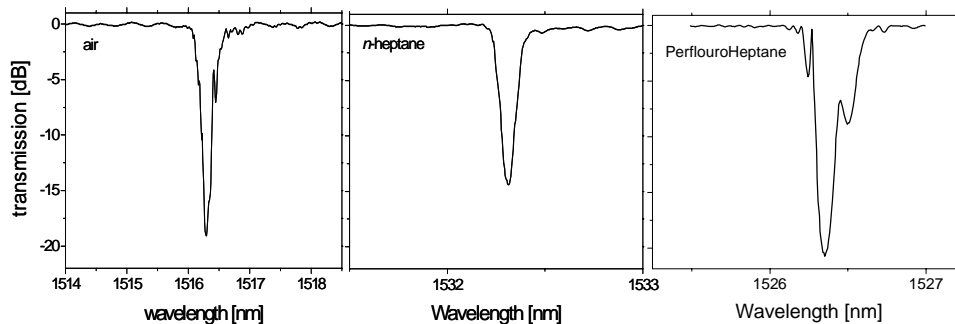


Fig. 3. Bragg grating transmission spectra within the photonic crystal fibre containing air and the two organic liquid samples. Clearly, when the index of the holes goes up the effective index of the grating goes up, resulting in a higher Bragg-wavelength for otherwise similar gratings.

The experimental approach involved using an exciplex 248nm pulsed laser (cumulative fluence at 248nm = 250mJ/cm²) to direct write gratings into the hydrogen loaded (150bar) germanosilicate core loaded with an optical phase mask ($\Lambda = 1069\text{nm}$). The hydrogen loading procedure was similar to that reported in [8] where a reservoir of molecular hydrogen is stored within the air holes by collapsing the ends of the fibre using a fusion splicer. Figure 3 shows the spectra of the grating with air, *n*-heptane and perfluoroheptane respectively. From the shift in Bragg wavelength, the resultant effective index difference between the air and *n*-heptane is determined to be $\Delta n = 15 \times 10^{-3}$ and between air and perfluoroheptane $\Delta n = 9.4 \times 10^{-3}$.

4. Composite Fibre Thermo-optic Coefficients

The effective thermo-optic coefficients of the fibre system can be experimentally determined directly from the measured shift in Bragg wavelength of the gratings as a function of temperature. Figure 4 shows the effective index extracted from the Bragg wavelength shift over the temperature range 25-100°C for the photonic crystal fibre with air, *n*-heptane and perfluoroheptane inside the holes. Since the fraction of optical field within the holes is also wavelength dependent, gratings were written in both the perfluoroheptane and heptane samples at both 1.5 and 1.0 μm . Table 2 shows the values for $\partial n_{\text{eff}} / \partial T$ obtained from the slopes of the effective index versus temperature plot for each sample. By tailoring the material thermo-optic coefficient and the Bragg wavelength, $\partial n_{\text{eff}} / \partial T$ can range from as little as $+2.5 \times 10^{-3}$ to as large as -45×10^{-3} . Consequently, the value can be adjusted, either positively or negatively, as required for a particular application. The Bragg wavelengths were restricted by the available phase mask but at 1.0 μm a reduction of $\partial n_{\text{eff}} / \partial T$ by a factor close to four has been achieved. If written at slightly longer wavelengths than 1.0 μm zero temperature dependence is possible. Numerical calculations suggest a value closer to 1.2 μm , is optimum

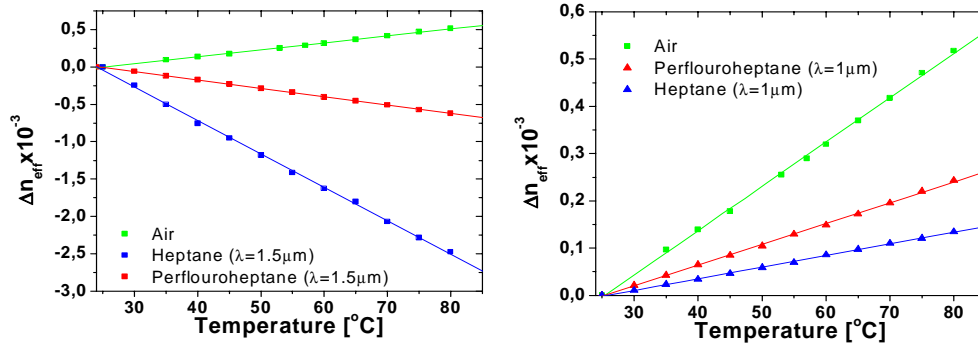


Fig. 4. Change in effective index, determined from the shift in Bragg wavelength as a function of temperature, for the photonic crystal fibre with three sample materials within its holes.

when perflouroheptane is used as liquid in the holes. The value for air is a little lower than that previously reported for a pure silica photonic crystal fibre [4] where the core size was much larger and the mode field within the holes was commensurately less.

An effective thermo-optic coefficient of zero has immense significance for many devices including the packaging of components such as fibre Bragg gratings and active devices such as DFB fibre lasers, which can experience some internal heating. One substantial area of benefit is sensing where the separation of strain and temperature has traditionally been extremely difficult to achieve often requiring complex interrogation or reference systems. Simply reversing the sign of the temperature dependence, or removing it all together, greatly simplifies the problem.

Overall, despite the small percentage of optical field within the holes, a significant change in thermo-optic coefficient of the photonic crystal fibre, ranging from positive to negative, has been demonstrated. The air-structure of the photonic crystal fibre clearly has a significant advantage in allowing control over such mechanical properties by permitting post control over the composite structure determined by the glass and the material within the holes. This is in contrast to traditional mechanisms involving the chemical composition of the material as a whole and makes full use of micro structuring, and potentially nano structuring, of the material. It means that many other parameters previously studied with structural designs, including dispersion and novel nonlinearities, can likewise be improved upon by controlling additional material incorporation in a selective and intentional manner. Given the wavelength dependence of the effective index, it does mean, however, that particular consideration of the structure, including size, number and distribution of holes, is done in parallel. The absorption properties of the media also need to be considered, especially in sensing applications.

Table 2. $\partial n_{\text{eff}}/\partial T$ for various composite fibre systems.

Liquid	$\partial n_{\text{eff}}/\partial T \times 10^{-3}$
Air ($\lambda_B = 1.5\mu\text{m}$)	9.4
Heptane ($\lambda_B = 1.5\mu\text{m}$)	-45
Perflouroheptane ($\lambda_B = 1.5\mu\text{m}$)	-11
Heptane ($\lambda_B = 1\mu\text{m}$)	2.5
Perflouroheptane ($\lambda_B = 1\mu\text{m}$)	4.4

5. General method for determining $\partial n/\partial T$ of a material

Using the measured value of the photonic crystal fibre temperature dependence with *n*-heptane inside the holes and inserting the appropriate parameters into equation 3, the actual temperature dependence of the refractive index of *n*-heptane is found to be $\partial n_{hept}/\partial T = -480 \times 10^{-6} \text{ } ^\circ\text{C}^{-1}$. This is within 4% that of [8] where $\partial n_{hept}/\partial T = -502 \times 10^{-6} \text{ } ^\circ\text{C}^{-1}$. The experimental variation between many reported measurements in the literature of $\partial n/\partial T$ is often larger. Provided the experimental parameters of the fibre and grating are well understood, the photonic crystal fibre device described here can be used to determine with reasonable accuracy the temperature dependent refractive index of any low-loss material placed within the holes. For example, the technique can be applied to determining $\partial n/\partial T$ of perfluoroheptane, for which we were unable to find a value within the wider literature. Perfluoroheptane differs from *n*-heptane only in the displacement of hydrogen atoms with fluorine atoms. Yet this is sufficient to alter the refractive index of the holes substantially (Table 1) and lead to a large change in $\partial n_{hept}/\partial T$. On the other hand, the value we determine for perfluoroheptane itself is $\partial n/\partial T = -468 \times 10^{-6} \text{ } ^\circ\text{C}^{-1}$ is only slightly lower than that of *n*-heptane. Thus the method is readily implemented and easy to carry out. More sophisticated applications would involve detailed studies of, for example, trends such as the observed decreasing temperature dependence with increasing alkane chain [7].

6. Conclusions

In conclusion, using a UV-inscribed Bragg grating the thermo-optic coefficient of a photonic crystal fibre with different materials inside the air holes has been characterised. Larger temperature tuneable gratings compared to conventional technologies are feasible, with the tuning direction and magnitude adjustable using appropriate materials. Alternatively, we have demonstrated that it is feasible to balance the temperature dependence of the silica and material within the hole to achieve a zero temperature dependence of the effective mode index. This allows a simple and direct alternative for separating out the thermal and strain coefficients that make up the response of numerous sensor devices as well as offering a way of achieving zero temperature dependent packaging. Such an elegant, low cost and simple approach utilises fully the differences between void-structured and conventional fibre technologies. We note and demonstrate that the method used here offers an alternative approach to characterising (and perhaps standardising) the refractive index of any medium that can be inserted with low loss into the holes of the structure. Finally, the work reported here is not confined to structured silica fibre and can be equally applied to other porous media or systems, including photonic crystal circuits and devices.